# Sequence Specific Mutagenesis of the Major (+)-anti -Benzo[ a ]pyrene Diol Epoxide−DNA Adduct at a Mutational Hot Spot in Vitro and in Escherichia coli Cells

**ARTICLE** *in* CHEMICAL RESEARCH IN TOXICOLOGY · APRIL 1997

Impact Factor: 3.53 · DOI: 10.1021/tx9601925 · Source: PubMed



**7 AUTHORS**, INCLUDING:

Manny D Bacolod
Weill Cornell Medical College
**24** PUBLICATIONS **706** CITATIONS
SEE PROFILE

Nicholas E Geacintov
New York University
**432** PUBLICATIONS **12,020** CITATIONS
SEE PROFILE

Edward L Loechler
Boston University
**64** PUBLICATIONS **2,683** CITATIONS
SEE PROFILE

Ashis Basu
University of Connecticut
**109** PUBLICATIONS **3,308** CITATIONS
SEE PROFILE

# *Articles*

## Sequence Specific Mutagenesis of the Major (+)-*anti*-Benzo[*a*]pyrene Diol Epoxide−DNA Adduct at a Mutational Hot Spot *in Vitro* and in *Escherichia coli* Cells

Christopher J. Hanrahan,[†,‡] Manny D. Bacolod,[†,‡] Rajeev R. Vyas,[†] Tongming Liu,[§] Nicholas E. Geacintov,[§] Edward L. Loechler,[||] and Ashis K. Basu*[,†]

*Department of Chemistry, University of Connecticut, Storrs, Connecticut 06269, Department of Chemistry, New York University, New York, New York 10003, and Biology Department, Boston University, Boston, Massachusetts 02215*

*Received November 25, 1996*[⊗]

In the *supF* gene, most (+)-*anti*-benzo[*a*]pyrene diol epoxide ((+)-*anti*-B[a]PDE) mutagenesis hot spots in *Escherichia coli* are in 5′-GG sequences [Rodriguez and Loechler (1993) *Carcinogenesis 14*, 373−383]. A major hot spot was detected at $G_1$ in the sequence 5′-GCG$_1$G$_2$-CCAAAG, whereas $G_2$ yielded very few mutants. In order to investigate the details of such sequence context effects of (+)-*anti*-B[a]PDE mutagenesis, we have constructed 25-mer oligonucleotides and single-stranded M13 genomes containing the above decamer sequence, in which the *trans*-$N^2$-dG adduct induced by (+)-*anti*-B[a]PDE [(+)-*trans*-*anti*-B[a]P-$N^2$-dG] at $G_1$ or $G_2$ was introduced. *In vitro* DNA synthesis on the adducted 25-mers was strongly blocked at each site, although the 3′ → 5′ exonuclease-deficient Klenow fragment could incorporate a nucleotide opposite the adduct in the presence of $Mn^{2+}$. For both sites purine nucleotides were preferred. The ratio $V_{max}/K_m$ indicated that the efficiency of incorporation of dGTP opposite these sites was very similar, but dATP incorporation opposite the adduct at $G_1$ was five-fold more efficient than that at $G_2$. For each site, further extension beyond the adducted nucleotide was investigated by annealing four different primers, in which only the nucleotide opposite the adducted deoxyguanosine was altered. Significant extension was only observed when deoxyadenosine was located opposite adducted $G_1$. When the M13 genomes containing the (+)-*trans*-*anti*-B[a]P-$N^2$-dG were replicated in *E. coli*, survival of each adducted genome was less than 1% as compared to the unadducted genome. Upon induction of SOS, viability increased 2−6-fold. DNA sequencing showed no base substitutions in the progeny from SOS-uninduced cells, although small deletions in a quasipalindromic sequence occurred with the adduct being located at either site. However, following SOS induction, up to 40% targeted base substitutions were detected when the adduct was located at $G_1$, while ∼12% of the progeny were mutants with the adduct at $G_2$. Most base substitutions were targeted G → T transversions. We conclude that (+)-*trans*-*anti*-B[a]P-$N^2$-dG is a highly mutagenic and replication blocking lesion. In addition, the biological consequence of this adduct depends on whether it is located at $G_1$ or $G_2$, suggesting that sequence context plays a major role in the mutagenic processing of this adduct.

### Introduction

The mutagenic and tumorigenic properties of benzo[*a*]pyrene (B[a]P[1]) metabolites have been studied extensively for the last three decades (for a review, see ref 1). B[a]P is metabolized to (+)- and (−)-B[a]P 7,8-dihydrodiol (*2*, *3*). (−)-B[a]P 7,8-dihydrodiol is tumorigenic in newborn mice whereas the (+) enantiomer shows little tumorigenic activity (4). (−)-B[a]P 7,8-dihydrodiol is further metabolized to (−)-*syn*- and (+)-*anti*-r-7,t-8-dihydroxy-t-9,10-epoxy-7,8,9,10-tetrahydrobenzo[*a*]pyrene (B[a]PDE) whereas (+)-B[a]P 7,8-dihydrodiol generates (+)-*syn*- and (−)-*anti*-B[a]PDE (*3*, *5*). The (+)-*anti*-B[a]PDE enantiomer is much more tumorigenic than (−)-*anti*-B[a]PDE (*6*, *7*). The mutagenic activity of these two enantiomers, however, are dependent on the type of assay used (8−11). Both (+)- and (−)-*anti*-B[a]PDE covalently bind to DNA, and the major adducts are formed at the C10 position of B[a]PDE by trans and cis addition of $N^2$-dG, the trans addition product (+)-*trans*-*anti*-B[a]P-$N^2$-

* Address correspondence to this author.
† University of Connecticut.
‡ These two authors contributed equally to this work.
§ New York University.
|| Boston University.
⊗ Abstract published in *Advance ACS Abstracts,* March 15, 1997.
[1] Abbreviations: B[a]P, benzo[*a*]pyrene; (+)-*anti*-B[a]PDE, (+)-r-7,t-8-dihydroxy-t-9,10-epoxy-7,8,9,10-tetrahydrobenzo[*a*]pyrene (anti); (+)-*trans*-*anti*-B[a]P-$N^2$-dG, trans addition product of (+)-*anti*-B[a]PDE at $N^2$ position of 2′-deoxyguanosine; KF (exo$^-$), 3′ → 5′ exonuclease-deficient Klenow fragment; Sequenase version 2.0, a modified 3′ → 5′ exonuclease-free T7 DNA polymerase; IPTG, isopropyl β-D-thiogalactopyranoside; X-gal, 5-bromo-4-chloro-3-indolyl β-D-galactopyranoside; ss, single stranded; ds, double stranded; Gua, guanine; Ade, adenine; Cyt, cytosine; Thy, thymine; dG, 2′-deoxyguanosine; dA, 2′-deoxyadenosine; dC, 2′-deoxycytidine.

S0893-228x(96)00192-0 CCC: $14.00 

dG being the predominant adduct (*12*−*17*).

Despite a large number of mutagenesis studies performed with B[a]PDE, it is uncertain which adducts are responsible for the observed mutagenicity. This is due, in part, to the use of racemic B[a]PDE in many studies, which generates several stereoisomeric adducts (*18*−*20*). In the limited number of studies that used optically pure (+)-*anti*-B[a]PDE, it is still uncertain whether the observed mutagenesis was due to the *cis* or the *trans* adducts (*21*−*24*). In recent years, site-specific adducted oligonucleotides and plasmid or viral vectors have been employed to investigate these types of mechanistic questions (*25*−*27*). Indeed, (+)-*trans*-*anti*-B[a]P-$N^2$-dG has been studied in *Escherichia coli*, and it was found to induce targeted G → T base substitutions in ∼1% progeny DNA (*28*). *In vitro* miscoding properties of stereoisomeric (+)- and (−)-*anti*-B[a]PDE adducts at $N^2$-dG have also been explored (*29*, *30*). In one *in vitro* study, Sequenase version 2.0 and human DNA polymerase α were strongly blocked by (+)-*trans*-*anti*- and (+)-*cis*-*anti*-B[a]P-$N^2$-dG, and only a small amount of dCMP was incorporated opposite these lesions (*29*). In another study in which 3′ → 5′ exonuclease-free Klenow fragment [KF (exo⁻)] was used, dAMP was preferentially incorporated opposite all four of the stereoisomeric B[a]PDE adducts (*30*). Efficiency of dATP misincorporation was 2 or 3 orders of magnitude higher for (−)-*trans*-*anti*-B[a]P-$N^2$-dG than for the other three stereoisomeric $N^2$-dG adducts. In this study one-, two-, and three-base deletion products were also detected.

An important issue that was not addressed in any of these studies is that B[a]P-$N^2$-dG mutagenesis may also be dependent on the site of carcinogen modification. Sequence context effects are believed to be important for mutagenesis of many carcinogen−DNA adducts (discussed in ref 27). For (+)-*anti*-B[a]PDE, an analysis of the mutational spectrum in *supF* gene of an *E. coli* plasmid revealed that many hot spots are located in 5′-GG sequences (where the underscored Gua is frequently mutated) (*23*). In order to investigate the effects of DNA polymerase on the same B[a]PDE-dG adduct, we have chosen a specific decamer sequence from the *supF* gene, 5′-GCG$_1$G$_2$CCAAAG, in which G$_1$ was detected to be a hot spot for mutagenesis with SOS, whereas G$_2$ yielded very few mutants. [In other studies (e.g., refs 23, 24, and 31), G$_1$ and G$_2$ are referred to as G$_{115}$ and G$_{116}$, respectively.] We have synthesized two oligonucleotides in which the (+)-*trans*-*anti*-B[a]P-$N^2$-dG was located either at G$_1$ or at G$_2$. In a prior study, these decamers were inserted into an *E. coli* plasmid, and the mutagenic effect of these adducts was studied *in vivo* (*31*). The adduct at G$_1$ induced all three targeted base substitutions, although GC → TA predominated. Semi-targeted mutations at G$_2$ were also observed. The adduct at G$_2$ was quantitatively less mutagenic than the adduct at G$_1$. To extend the previous *in vivo* study that was carried out in ds DNA, in the present work we have investigated the effects of these adducts on DNA synthesis *in vitro* by two 3′ → 5′ exonuclease-deficient DNA polymerases. We have chosen Sequenase, a replicative DNA polymerase from bacteriophage T7, for some of the studies, but the kinetics of incorporation were performed with KF (exo⁻). Although KF is primarily involved in DNA repair, it is a simple peptide with high fidelity. It does not require accessory proteins and is available as a highly pure enzyme. Indeed, it has been used extensively for steady-state kinetic studies of nucleotide incorporation opposite many carcinogen−DNA adducts. Finally, to complement the *in vitro* investigation, we have constructed ss bacteriophage M13 genomes containing the adduct at either G$_1$ or G$_2$. Viability and mutagenesis of these vectors in *E. coli* were studied.

## Materials and Methods

**Materials. Caution:** *B[a]P and its metabolites are carcinogenic to rodents and should be handled carefully.*

The 7*R*,8*S*-dihydroxy-9*S*,10*R*-epoxy-7,8,9,10-tetrahydrobenzo[*a*]pyrene [(+)-*anti*-B[a]PDE] was purchased from the National Cancer Institute Chemical Carcinogen Standard Repository (Lot No. 92-356-91-19). All other organic chemicals were from Aldrich Chemical Co. (Milwaukee, WI). [$\gamma$-$^{32}$P]- and [α-$^{35}$S]dATP were from Du Pont New England Nuclear (Boston, MA). T4 polynucleotide kinase and DNA ligase were obtained from Bethesda Research Laboratory (Gaithersburg, MD). 3′ → 5′ exonuclease-deficient Klenow fragment [KF (exo⁻)], a modified 3′ → 5′ exonuclease-free T7 DNA polymerase (Sequenase version 2.0), M13 DNA sequencing kit, and 5-bromo-4-chloro-3-indolyl $\beta$-D-galactopyranoside (X-gal) were purchased from Amersham Life Science Inc. (Arlington Hts, IL). Ethidium bromide, polyethylene glycol 8000, and isopropyl $\beta$-D-thiogalactopyranoside (IPTG) were obtained from Sigma Chemical Co. (St. Louis, MO).

*E. coli* strains GW5100 (JM103, P1⁻) and DL7 (AB1157, *lac*Δ*U169*, *uvr*⁺), in which the latter strain carries a chromosomal lac deletion, were obtained from G. Walker and J. Essigmann (MIT, Cambridge, MA), respectively.

**Methods.** HPLC separations of the oligonucleotides were performed using reverse-phase columns (Phenomenex Ultramex C-18, 4.6 × 250 mm). Bacteriophage M13mp7L2 DNA was prepared as described (*32*). Bacterial media (including SOC medium) were prepared according to Sambrook et al. (*33*).

**Synthesis of Adducted Oligonucleotides.** The decamers containing (+)-*trans*-*anti*-B[a]P-$N^2$-dG at either G$_1$ or G$_2$ has been synthesized as reported in Jelinsky et al. (*31*). A 5′-phosphorylated 15-mer, 5′-TAGAGATTGGTAGGG, was ligated to the modified decamers, 5′-GCG$_1$*G$_2$CCAAAG, 5′-GCG$_1$-G$_2$*CCAAAG (in which G* denotes the adducted Gua) and the unmodified control sequence 5′-GCGGCCAAAG in the presence of a 20-mer, 5′-ACCAATCTCTACTTTGGCCG, that was partially complementary to each of the ligating oligomers. A typical reaction contained 3 nmol equiv of each oligonucleotide. For annealing to occur, the mixture of oligonucleotides in 100 $\mu$L of 25 mM Tris-HCl (pH 7.5), 10 mM $MgCl_2$, and 5 mM DTT was heated at 80 °C for 5 min and slowly cooled to 4 °C over a 2-h period. T4 DNA ligase (5 units) and ATP (final concentration 1 mM) were added, and the mixture was incubated at 16 °C overnight. The reaction was stopped by the addition of an equal volume of bromophenol blue−xylene cyanol dye mixture containing formamide (95%) and EDTA (12 mM). The ligated 25-mer was separated on a 16% polyacrylamide−8 M urea gel. The oligonucleotides were visualized by UV shadowing and excised (*34*). The product was eluted in 1× TE buffer and desalted on a C-18 Sep-Pak cartridge (Waters).

**DNA Polymerase Reaction.** Oligonucleotide primers, 5′-CCCTACCAATCTCTA (15-mer), 5′-CCCTACCAATCTCTACTT-TGG (20-mer), 5′-CCCTACCAATCTCTACTTTGGC (21-mer), and a set of four 22-mers 5′-CCCTACCAATCTCTACTTTGGN or 23-mers 5′-CCCTACCAATCTCTACTTTGGCN (in which N = G, C, T, or A), were end-labeled with [$\gamma$-$^{32}$P]ATP in the presence of T4 polynucleotide kinase and purified on a C-18 Sep-Pak cartridge as described (*34*). A primed template was obtained by annealing 5′-$^{32}$P-labeled 15-mer primer (2 pmol) to modified or unmodified 25-mer template (5 pmol) in 10 mM Tris-HCl (pH 7.4) and 0.1 mM EDTA. To ensure quantitative annealing of the 22- and 23-mer primers used for extension studies a 10-fold excess template (20 pmol) was used. The mixture was heated at 65 °C for 10 min and cooled slowly to 4 °C. A mixture of dNTPs, the concentration of which varied for each experiment, was added. KF (exo⁻) (2−10 units) was

incubated in 50 mM Tris-HCl (pH 8.0), 8 mM $MgCl_2$, 2 mM DTT, and BSA (100 $\mu$g/mL). For Sequenase version 2.0 (1−2 units), the buffer used was 36 mM Tris-HCl (pH 7.5), 0.1 mM EDTA, 8 mM $MgCl_2$, 50 mM NaCl, and 1 mM DTT. For certain experiments with KF (exo$^-$) and Sequenase, 8 mM $MgCl_2$ was replaced with 0.5 mM $MnCl_2$. After the desired time of incubation at 37 °C, 5 $\mu$L of stop solution (95% formamide, 20 mM EDTA, 0.05% bromophenol blue, 0.05% xylene cyanol) was added. After denaturing at 90 °C for 2 min, a portion was loaded on to a 30 cm × 40 cm × 0.4 mm gel consisting of 16% acrylamide/*N,N*′-methylenebis(acrylamide) (19:1) containing 8 M urea and was electrophoresed in 45 mM Tris borate, pH 8.25, and 1.25 mM EDTA.

Kinetic data of nucleotide incorporation opposite the lesion and further extension was determined with KF (exo$^-$) (5 units) at 37 °C by the method of Goodman and co-workers (*35*). For the insertion kinetics, the optimal concentrations of dCTP (for the adduct at $G_1$) and dGTP (for the adduct at $G_2$) were determined to be 100 and 10 $\mu$M, respectively. Following the time course studies, a 5-min incubation time for both insertion and chain extension was chosen. All reactions were linear during the course of these experiments. The Michaelis constant ($K_m$) and maximum rate of reaction ($V_{max}$) were extrapolated from a Hanes−Woolf plot of the kinetic data. Data in Table 1 represent an average of 4−6 independent experiments.

Construction of M13 genomes containing a single (+)-*trans-anti*-B[a]P-$N^2$-dG. Single-stranded (ss) M13mp7L2 was linearized by extensive digestion with *Eco*RI (i.e., 8 units of the restriction endonuclease were used per microgram of DNA, and following ethanol precipitation, the digestion step was repeated). The linearized M13 DNA was converted to a gapped circular molecule by annealing a 5-fold molar excess of a 49-mer scaffold oligonucleotide at a concentration of 100 ng/$\mu$L in 25 mM NaCl. The gapped section of the 49-mer scaffold was complementary to the decamer 5′-GCGGCCAAAG. One hundred-fold molar excess of a 5′-phosphorylated adducted decamer (or the control oligonucleotide) was ligated into the gap at 16 °C for 48 h in the presence of 20 units of T4 DNA ligase.

To visualize the unmodified and modified DNA constructs, a portion of each of these genomes was run on an 1% agarose gel in the presence of ethidium bromide. Since the migration characteristics of linear and circular DNA in an agarose gel is different, we could quantitate the extent of ligation of the 10-mer to both ends of the gap as we have done in a prior study (*32*). It is worth noting that ligation of the two ends of the gap in the absence of an appropriate 10-mer did not exceed 1% (data not shown).

**Transformation in *E. coli*.** Transformations were carried out as reported in Malia et al. (*32*). Briefly, *E. coli* cells (DL7) were grown in 100-mL cultures to 1 × $10^8$ cells/mL and then harvested by centrifugation at 5000*g* for 15 min at 0 °C. The cells were resuspended in equal volume ice-cold deionized water and recentrifuged at 5000*g* for 30 min. This procedure was repeated except the cells were resuspended in 50 mL of water. The bacterial pellet was resuspended in 1 mL of glycerol/water (10% v/v) and kept on ice until further use. To induce SOS, the following additional steps were introduced after the first centrifugation. The cells were resuspended in 50 mL of 10 mM $MgSO_4$ and treated with UV light (254 nm) (20 J/m$^2$) in 25-mL aliquots in 150 × 50 mm plastic Petri dishes. The cultures were incubated in Luria broth at 37 °C for 40 min in order to express SOS functions maximally. Following SOS induction, these cells were centrifuged, deionized, and resuspended in glycerol/water in a similar manner as described earlier except all manipulations were carried out in subdued light.

In order to remove the 49-mer scaffold from the M13 DNA, each DNA solution was heated at 100 °C for 1 min and rapidly cooled to 0 °C. Prior to heating, a 10-fold molar excess of a 49-mer that contained the DNA sequence complementary to the scaffold oligomer was added to the DNA solution to prevent the scaffold to reanneal on the M13 DNA. For each transformation, 50 $\mu$L of the cell suspension was mixed with 4 $\mu$L (500 ng) of DNA solution and transferred to the bottom of an ice-cold Bio-Rad Gene-Pulser cuvette (0.1 cm electrode gap). On the basis of ligation efficiency of the oligonucleotides, the same amount of circular genome of the control and two modified genomes was used for transformation, even though the amount of linearized DNA was different for different constructs (see Results). (Linearized genome did not yield any plaque at the concentrations (∼500 ng) transfected in these experiments.) Electroporation of cells was carried out in a Bio-Rad Gene-Pulser apparatus at 25 $\mu$F and 1.8 kV with the pulse controller set at 200 Ω. Immediately after electroporation, 1 mL of SOC medium was added, and the mixture was transferred to a 10-mL culture tube. Part of the cells was plated following a 30-min recovery at 37 °C in the presence of the plating bacteria *E. coli* GW5100, IPTG, and X-gal to determine the number of independent transformants. The remainder of cells were centrifuged at 15000*g* for 5 min to isolate the phage-containing supernatant.

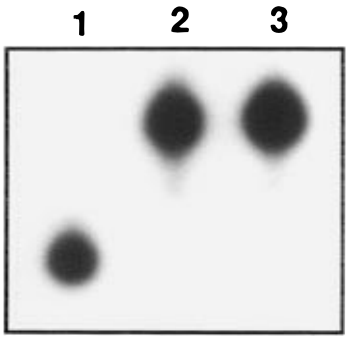


**Figure 1.** Polyacrylamide gel electrophoresis of $^{32}$P-end labeled (+)-*trans-anti*-B[a]P-$N^2$-dG-modified and unmodified 25-mers. Lane 1 shows the unmodified 25-mer, whereas lanes 2 and 3 contained the 25-mers with the adduct at $G_2$ and $G_1$, respectively, following electrophoresis at 1800 V for 5.5 h. Relative migration of the modified 25-mers in lanes 2 and 3 as compared to the unmodified 25-mer in lane 1 was estimated to be ∼92%.

## Results

**Oligonucleotides Containing (+)-*trans-anti*-B[a]P-$N^2$-dG.** Synthesis of the decamers containing (+)-*trans-anti*-B[a]P-$N^2$-dG at either $G_1$ or $G_2$ has been reported (*31*). The modified 10-mers and the unmodified control 10-mer were ligated to a 5′-phosphorylated 15-mer, 5′-TAGAGATTGGTAGGG, in the presence of T4 DNA ligase and a 20-nucleotide complementary oligomer, 5′-ACCAATCTCTACTTTGGCCG, which held the ligating oligonucleotides together. The resultant 25-mers, 5′-GCG$_1$G$_2$CCAAAGTAGAGATTGGTAGGG with the adduct at either $G_1$ or $G_2$, and their unmodified counterpart were purified by electrophoresis on a denaturing polyacrylamide gel. Analysis of the 25-mers was performed by $^{32}$P-end labeling of a fraction of the oligonucleotides followed by polyacrylamide gel electrophoresis and autoradiography, which showed slower mobility of the adducted 25-mers compared to the unmodified control, as expected (Figure 1). It is noteworthy that the adducted 25-mers did not contain any visible contamination (>2%) of the unmodified 25-mer.

***In Vitro* DNA Replication System.** We studied the ability of KF (exo$^-$) and Sequenase to replicate past (+)-*trans-anti*-B[a]P-$N^2$-dG adduct *in vitro*. The replication system used the following primed template in which the adducted nucleotide was located at either $G_1$ or $G_2$:

15-mer primer 3'- ATCTCTAACCATCCC$^{32}$p -5'

25-mer template 5'- GCG$_1$G$_2$CCAAAGTAGAGATTGGTAGGG -3'

The template was hybridized to a 5′-$^{32}$P-labeled complementary 15-mer primer. The adduct was located at

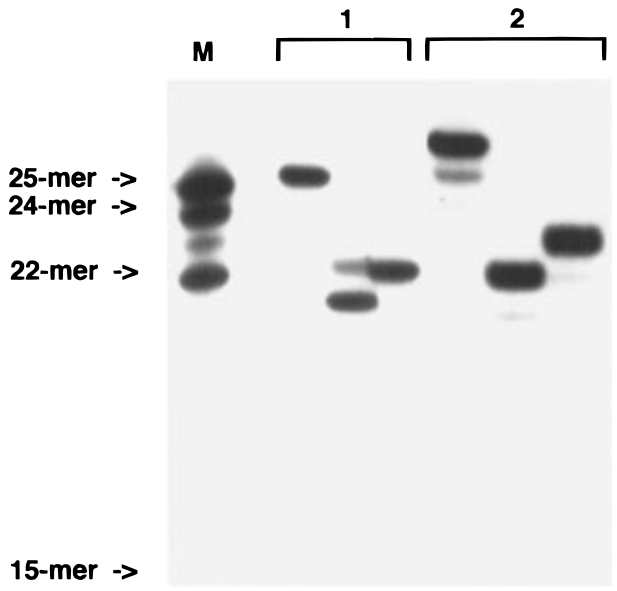


**Figure 2.** Polyacrylamide gel electrophoresis separation of DNA fragments generated by extension of $^{32}$P-end labeled 15-mer primer on unmodified and (+)-*trans-anti*-B[a]P-$N^2$-dG-modified 25-mer templates. Polymerization was catalyzed by KF (exo$^-$) with $Mg^{2+}$ (panel 1) or $Mn^{2+}$ (panel 2) for 2 h. Each set of three lanes shows primer extension on unmodified, $G_2$- and $G_1$-modified templates, respectively. M shows the migration characteristics of the oligonucleotide standard.

template position 22 or 23 from the 3′-end, and the 3′-terminus of the primer was six or seven nucleotides away from the adduct site in the template as shown above. We have analyzed the products of DNA synthesis by using denaturing polyacrylamide gel electrophoresis. For each experiment, a control template was replicated in a similar manner.

**Replication Block by (+)-*trans-anti*-B[a]P-$N^2$-dG.** With KF (exo$^-$), DNA synthesis was blocked at the nucleotide 3′ to the adduct site even after a 2-h incubation (Figure 2). By contrast, the unmodified template produced full-length 25-nucleotide product within 1 min. After 2 h the primer was extended predominantly to a mixture of 25- and 26-mers. It is likely that nontemplated dATP incorporation occurred at the end of the extended primer as originally reported by Clark (*36*). The replication block 3′ to the adduct site was nearly quantitative for the adduct at $G_1$, and neither the concentration of dNTPs (from 100 $\mu$M to 1 mM) nor the concentration of DNA polymerase (2−10 units) influenced the amount of postlesion synthesis products to a significant extent (data not shown). For the adduct at $G_2$, partial nucleotide incorporation opposite the adduct occurred with KF (exo$^-$) (Figure 2, panel 1, second lane). Nevertheless, less than 1% full-length product was detected for each adducted template. Replacement of $Mg^{2+}$ with $Mn^{2+}$ has been shown to increase postlesion synthesis of many types of DNA damage (*37*−*39*). With KF (exo$^-$), significant incorporation opposite the adduct occurred at both sites (Figure 2, panel 2), although complete extension product did not exceed 2%. With Sequenase, however, the replication block prior to each of the adduct sites was nearly quantitative, and even in the presence of $Mn^{2+}$ further extension of the primer was not observed following a 2-h incubation (data not shown).

We monitored the time course of incorporation of a nucleotide opposite the adduct by KF (exo$^-$) with the 15-mer primer in the presence of all four dNTPs (Figure 3). In 2−3 min the 15-mer primer was extended nearly quantitatively to positions 21 and 22 for $G_1$ and $G_2$, respectively, which are on the 3′ side of each adduct site. Thereafter, there is a slow but steady increase of incorporation opposite the adduct in each case over a 2-h period with a maximum incorporation of ∼40%. With $Mn^{2+}$, the rate of incorporation was faster and virtually all of the primers had incorporated opposite the adduct at each site within ∼20-min. In contrast to the results in Figure 2, there was no major difference in the pattern of incorporation at $G_1$ vs $G_2$ with either $Mg^{2+}$ or $Mn^{2+}$.

**Nucleotide Incorporation Opposite (+)-*trans-anti*-B[a]P-$N^2$-dG.** In the presence of $Mn^{2+}$, significant nucleotide incorporation opposite the adduct at both $G_1$ and $G_2$ sites was observed with KF (exo$^-$) (Figures 2 and 3). To investigate the kinetics of incorporation of individual dNTPs opposite the adduct, a 21-mer and 20-mer primer were used on templates containing (+)-*trans-anti*-B[a]P-$N^2$-dG at positions $G_1$ and $G_2$, respectively. The Michaelis constant ($K_m$) and maximum rate of reaction ($V_{max}$) were derived from a Hanes−Woolf plot of the kinetic data by the method of Goodman and co-workers (*35*). Representative data are presented in Figure 4. Kinetic data were collected for dAMP and dGMP incorporation opposite the adduct either at $G_1$ or $G_2$ in the presence of $Mn^{2+}$ (Table 1). Incorporation of dCMP and dTMP was so sluggish that we were unable to obtain reproducible results. To avoid the possibility of substrate inhibition, we did not use substrate concentrations above 5 mM. It is interesting to note that the ratio $V_{max}/K_m$ indicated that the efficiency of incorporation of dGMP opposite sites $G_1$ and $G_2$ and dAMP opposite $G_2$ were very similar, but dAMP incorporation opposite the adduct at $G_1$ was 5-fold more efficient than that at $G_2$ (Table 1).

**Table 1. Kinetic Parameters for dATP and dGTP Insertion Reactions Catalyzed by KF (exo$^-$)[a]**

| dNTP | adduct at | $V_{max}$ (%/min) | $K_m$ ($\mu$M) | $V_{max}/K_m$ |
|---|---|---|---|---|
| A | $G_1$ | 1.4 ± 0.3 | 9.4 ± 3.0 | 0.15 ± 0.01 |
| A | $G_2$ | 0.84 ± 0.08 | 30 ± 2 | 0.03 ± 0.003 |
| G | $G_1$ | 0.69 ± 0.06 | 28 ± 5 | 0.02 ± 0.002 |
| G | $G_2$ | 1.1 ± 0.1 | 35 ± 6 | 0.03 ± 0.01 |

[a] $K_m$ and $V_{max}$ were determined from Hanes−Woolf plots as described in Materials and Methods.

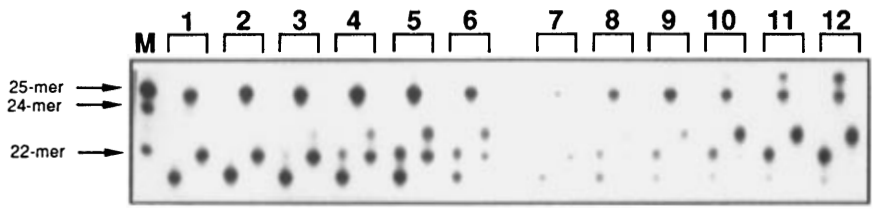


**Figure 3.** Time course of nucleotide incorporation opposite (+)-*trans-anti*-B[a]P-$N^2$-dG by KF (exo$^-$) at 100 $\mu$M concentration of all four dNTPs in the presence of $Mg^{2+}$ (1−6) or $Mn^{2+}$ (7−12). Each set of three lanes shows primer extension on $G_2$-modified, unmodified, and $G_1$-modified templates, respectively. For 1−6, the incubation times were 8, 16, 30, 60, 90, and 120 min. For 7−12, the incubation times were 4, 6, 8, 10, 15, and 20 min. M shows the migration characteristics of the oligonucleotide standard.

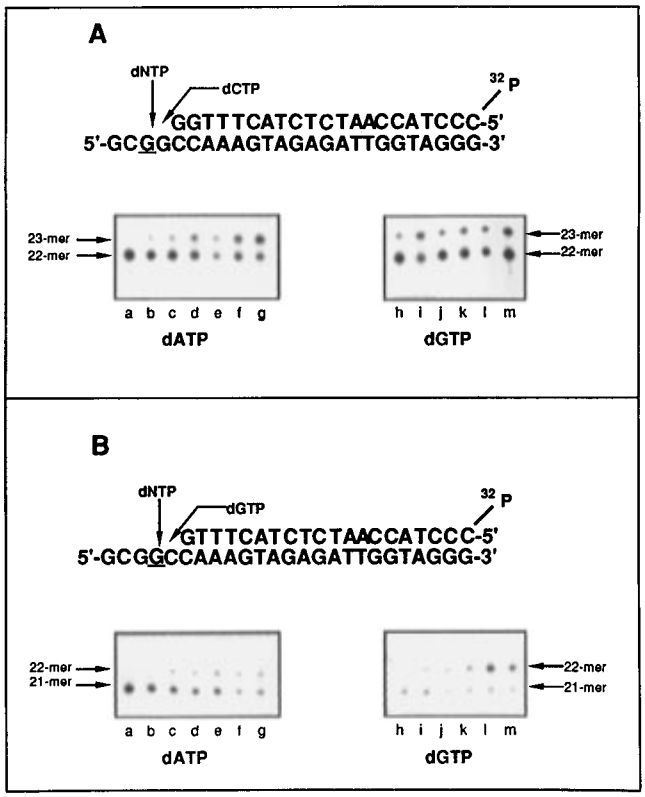


**Figure 4.** Representative autoradiogram of kinetic studies catalyzed by KF (exo⁻) showing gel band intensities as a function of dATP or dGTP substrate concentration. In panel A for the $G_1$-modified template, a 21-mer primer was annealed, and dCTP concentration was present at a constant concentration of 100 $\mu$M, which does not contribute measurable intensity to the 23-mer band. Likewise, in panel B, a 20-mer primer was annealed to the $G_2$-modified template, and dGTP concentration was present at a constant concentration of 10 $\mu$M. In each frame, lanes a−g represent dATP concentrations of 0, 8.5, 17, 25.5, 34, 42.5, and 51 $\mu$M, whereas lanes h−m show dGTP concentration of 33, 66, 99, 132, 165, and 198 $\mu$M.

To determine the rate of extension following incorporation of a nucleotide opposite the adduct, four separate 23-mer and 22-mer primer−template complexes were generated for the adduct at $G_1$ and $G_2$, respectively. Extension of each primer was monitored in the presence of increasing concentrations of dGTP for the adduct at $G_1$ and dCTP for the adduct at $G_2$. As shown in Figure 5, extension was only detectable when dA was located opposite the adduct at $G_1$ (frame A, lane 6). None of the other primer−template complexes showed any extension. These results show that, for both incorporation and extension of the primer, dA was evidently preferred opposite the adduct at $G_1$. For the same adduct at $G_2$, no detectable extension was observed with each of the four different primers (Figure 5, panel B). With the exception of dA opposite $G_1$, no chain extension was observed, even at a high concentration of dCTP with $G_1$ or dGTP with $G_2$. As a result, we were unable to determine the $V_{max}$ and $K_m$ values for the chain extensions.

**Table 2. Viability of (+)-*trans-anti*-B[a]P-$N^2$-dG Modified M13 in *E. coli*[a]**

| | relative survival (%) | | | | | |
|---|---|---|---|---|---|---|
| | | | adducted | | | |
| | control | | $G_1$ | | $G_2$ | |
| expt no. | −SOS | +SOS[b] | −SOS | +SOS[b] | −SOS | +SOS[b] |
| 1 | 100 ($3.3 \times 10^8$)[c] | 100 ($6.9 \times 10^6$)[c] | 0.11 | *d* | 0.42 | 0.77 |
| 2 | 100 ($4.6 \times 10^6$) | 100 ($6.7 \times 10^5$) | 0.03 | *d* | 0.27 | 1.2 |
| 3 | 100 ($1.0 \times 10^9$) | 100 ($9.8 \times 10^7$) | 0.21 | 1.2 | 0.17 | 1.2 |
| 4 | 100 ($8.3 \times 10^7$) | 100 ($1.3 \times 10^7$) | 0.20 | 0.40 | 0.61 | 1.6 |
| 5 | 100 ($8.4 \times 10^7$) | 100 ($5.0 \times 10^6$) | *d* | 0.62 | 0.04 | 0.06 |
| 6 | 100 ($3.9 \times 10^8$) | 100 ($9.8 \times 10^7$) | 0.18 | 1.3 | 0.54 | 0.18 |
| 7 | 100 ($2.2 \times 10^8$) | 100 ($2.6 \times 10^8$) | 0.08 | 0.37 | 0.10 | 0.22 |

[a] Viability (in percent) was determined by comparing the number of infective centers from the adducted DNA with that of the control genome (assumed to be 100% viability). [b] SOS was induced by UV (20 J/m$^2$) irradiation as described in Materials and Methods. [c] Transformation efficiencies (per $\mu$g of DNA) are shown in parentheses for the control genome. [d] No plaques were detected.

**Construction and Characterization of ss M13 Genomes Containing (+)-*trans-anti*-B[a]P-$N^2$-dG.** To investigate whether the biological effects of the adducts at these two sites are different in cells, we have constructed bacteriophage M13 genomes containing the adduct at either $G_1$ or $G_2$. Construction and characterization of the genomes containing (+)-*trans-anti*-B[a]P-$N^2$-dG at either $G_1$ or $G_2$ and a control have been carried out as we have done in a prior study (*32*). The efficiency of recircularization of the unmodified, $G_1$-modified, $G_2$-modified vectors were ∼30%, ∼30%, and ∼15%, respectively. Accordingly twice as much of the $G_2$-modified vector was used in transformations. The 49-mer scaffold was removed by a procedure we have used previously (*32*).

In a separate experiment, the adducted decamer was exposed to the conditions of ligation and denaturation of the scaffold. No detectable (<1%) degradation of the adducted oligonucleotide was noted, as determined by gel electrophoresis, suggesting that (+)-*trans-anti*-B[a]P-$N^2$-dG-modified DNA is stable to the conditions of genome construction.

**(+)-*trans-anti*-B[a]P-$N^2$-dG Is Highly Genotoxic in *E. coli*.** As shown in Table 2, in most transformations the viability of M13 genomes containing a single adduct was less than 1% in *E. coli* cells (DL7) with normal repair functions. The genotoxic effect of the adduct was so pronounced that in some experiments, particularly when the transformation efficiency was less than optimal, we failed to detect any progeny phage from the adducted genomes (Table 2). This suggests that (+)-*trans-anti*-B[a]P-$N^2$-dG constitutes a very strong block of DNA replication at least in the $G_1$ and $G_2$ sequence context. With SOS (20 J/m$^2$), a 2−6-fold increase in survival was

**Table 3. DNA Sequence Analysis of Progeny Phage[a]**

| | | control | | | | | $G_1$* | | | | | $G_2$* | | | | |
|---|---|---|---|---|---|---|---|---|---|---|---|---|---|---|---|---|
| expt no.[b] | SOS[c] | G | A | T | C | Del | G | A | T | C | Del | G | A | T | C | Del |
| **3** | − | ND[d] | − | − | − | − | 10/10 | − | − | − | − | 9/9 | − | − | − | − |
| | + | 17/17 | − | − | − | − | 10/23 | − | 9/23 | − | 4/17[e] | 18/21 | − | 3/21 | − | − |
| **6** | − | ND[d] | − | − | − | − | 5/7 | − | − | − | 2/7[f] | 8/9 | − | − | − | 1/9[f] |
| | + | 17/17 | − | − | − | − | 28/37 | − | 7/37 | 2/37 | − | 23/30 | − | 3/30 | − | 4/30[g] |

[a] Randomly selected progeny phage were subjected to DNA sequencing. [b] Experiment number denotes the appropriate experiment from Table 2. [c] SOS was induced by UV (20 J/m$^2$) irradiation as described in Materials and Methods. [d] Not determined. [e] Deletions of 5′-$G_1G_2$CCAA (2) and 5′-TGGC$G_1G_2$CCAAAG (2). [f] Deletions of 5′-CCAAAG. [g] Deletions of 5′-CCAAAG (3) and 5′-GC$G_1G_2$CCAAA (1).

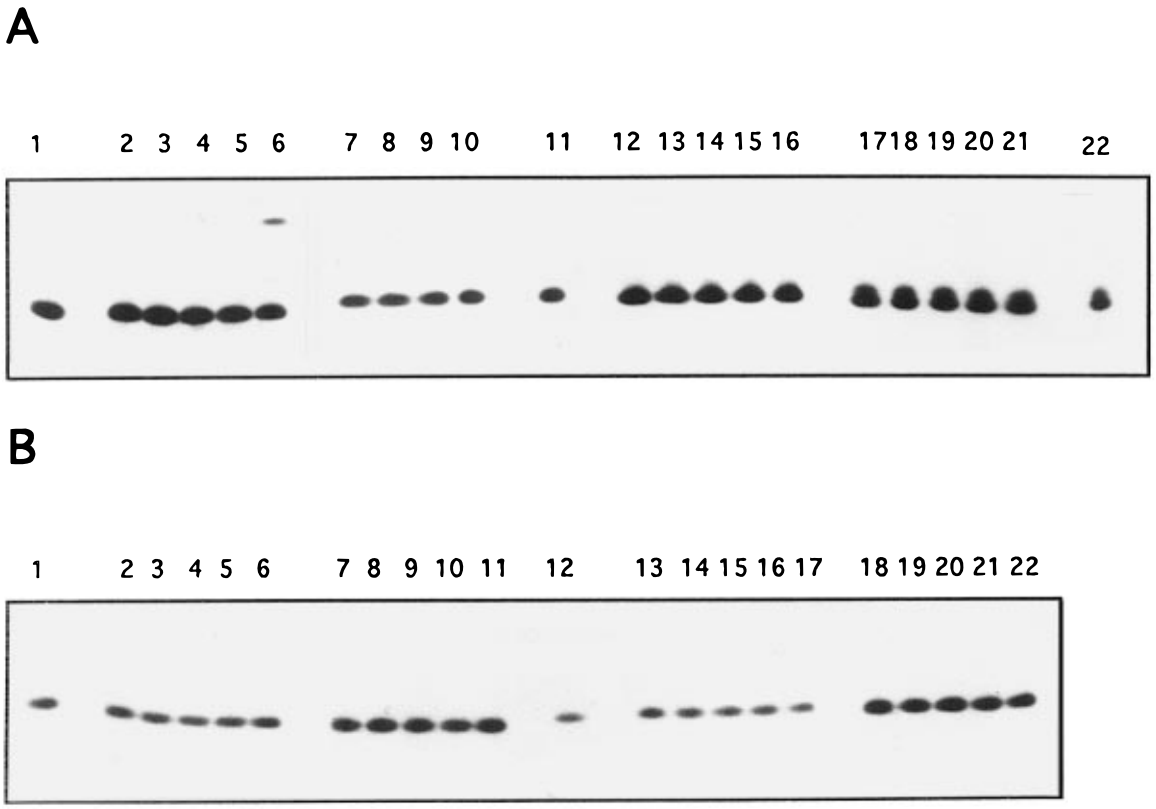


**Figure 5.** Autoradiogram of chain extension by KF (exo$^-$). Panel A: 23-mer primer containing A (lanes 2−6), G (lanes 7−11), C (12−16), and T (17−21) at the 3′ end annealed on to the $G_1$-modified template. Primer extension was catalyzed by KF (exo$^-$) (5 units) with 0.02, 0.05, 0.2, 0.5, and 1 mM dGTP. Lanes 1 and 22 show migration characteristics of the A-primer and T-primer, respectively. Panel B: 22-mer primer containing A (lanes 2−6), G (lanes 7−11), C (13−17), and T (18−22) at the 3′ end annealed on to the $G_2$-modified template. Primer extension was catalyzed by KF (exo$^-$) (5 units) with 0.05, 0.2, 0.5, 1, and 5 mM dCTP. Lanes 1 and 12 show migration characteristics of the A-primer and C-primer, respectively. It is noteworthy that in lane 6 extension of the 23-mer primer occurred predominantly to a 25-nucleotide product.

observed, which suggests that translesion bypass was more efficient with SOS. Since the progeny yield from the adducted vectors was low and some transformations did not generate any progeny phage, there is considerable uncertainty in the values for survival. Nevertheless, the average progeny of 0.12% and 0.31% without SOS when the adduct was at $G_1$ and $G_2$, respectively, may suggest a higher genotoxicity of the adduct at $G_1$. However, with SOS, the difference between average progeny yield of 0.56% and 0.75% with the adduct at $G_1$ and $G_2$, respectively, may not be statistically significant.

**Sequence-Specific Effects of (+)-*trans-anti*-B[a]P-$N^2$-dG Mutagenesis in *E. coli*.** Progeny phage from the transformations involving two different constructions were subjected to DNA sequencing (Table 3). No mutations in the progeny phage from the control were detected. By contrast, each adducted genome-generated progeny phage containing targeted base substitutions or small deletions. The small deletions occurred both with and without SOS, which included 6−12 base deletions as shown in Table 3. We suspect that a fraction of these deletions could have resulted following the formation of a quasipalindromic loop as shown in Scheme 1. It is conceivable that (+)-*trans-anti*-B[a]P-$N^2$-dG promotes formation of such loops, thereby increasing the frequency of small deletions, although it is unclear exactly what the driving force for this process is. It is noteworthy that the control genomes from several independent experiments did not induce these mutations. In addition to small deletions, (+)-*trans-anti*-B[a]P-$N^2$-dG induced SOS-dependent base substitutions at a high frequency with a strong bias toward G → T transversions. The adduct at

**Scheme 1**

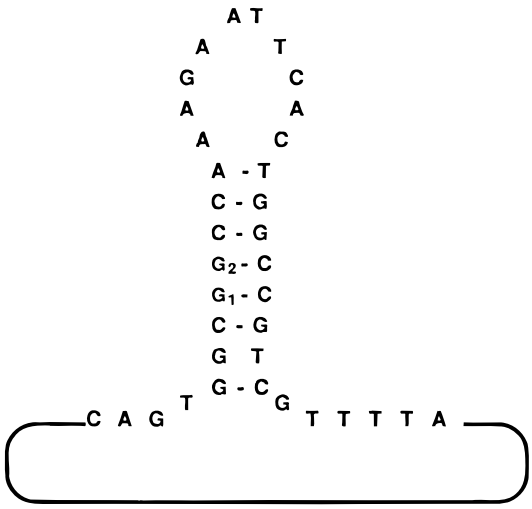


$G_1$ and $G_2$ exhibited base substitutions at a frequency of 18/60 (30%) and 6/51 (12%), respectively. Since the frequency of base substitutions at $G_1$ and $G_2$ was consistent from two completely independent experiments (which included different batches of adducted oligonucleotides, DNA constructs, and cells), the difference in mutagenesis due to the sequence context effect of (+)-*trans-anti*-B[a]P-$N^2$-dG is probably significant (Table 3). Base substitutions were almost exclusively G → T transversions. It is conceivable that G → C and G → A substitutions occur at a low frequency, since in one transformation with the adduct at $G_1$ we observed 2/37 G → C transversions,

although this result is not statistically significant because of the small number of phage analyzed.

## Discussion

Carcinogen-induced mutational hot spots occur due to one or more of the following: hot spot for adduction, cold spot for repair, and hot spot for errors during replication. Evidently the location of hot spots will depend on the DNA polymerases and a variety of cellular factors. In the current work, we investigated the misincorporation potential of the same adduct at two adjacent sites during translesion synthesis using an approach that eliminates the effect of differential binding and most likely the effect of DNA repair, since adduct repair could not take place in the *in vitro* replication assay, and the use of a ss vector would preclude nucleotide excision repair in cells.

As noted in two other studies (*29*, *30*), (+)-*trans*-anti-B[a]P-$N^2$-dG constituted a very strong block of DNA replication *in vitro*, and the DNA synthesis was predominantly terminated 3′ to the adducted nucleotide (Figure 2). Only a small amount of nucleotide incorporation occurred opposite the adduct (Figures 3 and 4), and even a smaller extension beyond the adduct site was detected (Figure 5). The incorporation opposite the adduct increased significantly in the presence of $Mn^{2+}$ (Figures 2 and 3). KF (exo$^-$) appears to discriminate between $G_1$ and $G_2$ based on the fact that both insertion of dAMP opposite the adduct and further extension with dA opposite the adduct were much more efficient when the adduct was located at $G_1$ (Figures 3−5, Table 1). It is also noteworthy that incorporation of dCMP as well as further extension with dC opposite the adduct at either site were particularly inefficient (Figures 4 and 5). Preferential insertion and extension with dA opposite (+)-*trans*-anti-B[a]P-$N^2$-dG was also shown in the prior *in vitro* study using KF (exo$^-$) (*30*). This bias may be related to the three-dimensional orientation of the adducted nucleotide, which is expected to influence its mode of base pairing (*42*). These data do not rule out, however, that (+)-*trans-anti*-B[a]P-$N^2$-dG may behave like a non-instructional lesion, across from which incorporation of dAMP is thought to occur (*38*, *39*).

Although DNA polymerase III rather than KF is the replicative polymerase in *E. coli*, our results showed that the adduct constituted an exceptionally strong block of DNA replication in cells where DNA polymerase III is probably involved. One percent or less progeny was obtained regardless of whether the adduct was at $G_1$ or $G_2$ (Table 2). When SOS functions of the host cells were induced, the viability of these genomes was increased several-fold. It is important to reiterate that the genotoxic effect of (+)-*trans-anti*-B[a]P-$N^2$-dG in ss DNA appears to be remarkably potent, since none of the other lesions tested in this system by us (*32*) or others (*40*, *41*, *43*) have induced such a strong effect on viability, especially when the SOS functions were induced. For example, a single T−T cyclobutane dimer reduced progeny to 0.4%−1.2%, but survival increased to ∼30% with SOS (*40*). Abasic sites reduced survival to 0.1%−0.7%, which increased to 5%−7% with SOS (*41*). Viability of stereoisomeric B[a]PDE−Ade adducts ranged from 6% for the (−)-*anti-trans*-B[a]PDE adduct to 23% for the (+)-*anti-cis*-B[a]PDE adduct (*43*). In our laboratory, *N*-(guanin-8-yl)-1-aminopyrene, the bulky C8 Gua adduct formed by 1-nitropyrene, constructed in a similar manner as in the current investigation, provided viability of 30−50% (*32*). We believe that the exceptionally high genotoxicity of (+)-*trans-anti*-B[a]P-$N^2$-dG has a profound impact on repair and mutagenesis of the adduct in ds DNA (*vide infra*).

Although we have sequenced only a limited number of progeny phage, several conclusions can be drawn. First, (+)-*trans-anti*-B[a]P-$N^2$-dG might induce small deletions in this sequence (Table 3), although it is hard to rule out the possibility that these were derived during the genetic engineering manipulations. Second, induction of SOS was a necessary prerequisite of (+)-*trans-anti*-B[a]P-$N^2$-dG-induced targeted base substitutions. SOS induction has been shown to enhance base substitutions by this adduct in several other studies (*28*, *31*). Third, (+)-*trans-anti*-B[a]P-$N^2$-dG is highly mutagenic in *E. coli*. (+)-*trans-anti*-B[a]P-$N^2$-dG is indeed highly mutagenic when compared with the stereoisomeric B[a]-PDE−Ade adducts that induced A → G mutations at frequencies ranging from 0.26% to 1.20% in ss DNA (*43*). Fourth, the frequency of base substitutions showed a marked difference between the locations $G_1$ and $G_2$; targeted base substitutions occurred at ∼30% and ∼12% frequency with the adduct at $G_1$ and $G_2$, respectively. Fifth, G → T transversions were the major type of mutations with SOS. A significantly higher frequency of G → T transversions at $G_1$ as compared to $G_2$ is consistent with our *in vitro* results. An important difference, however, is that deoxycytidine was incorporated opposite (+)-*trans-anti*-B[a]P-$N^2$-dG preferentially in cells, whereas KF (exo$^-$) preferred the purine nucleotides opposite the adduct *in vitro*.

Could the G → T transversions observed in this study be due to a contaminating oligonucleotide? Although the adducted oligonucleotides have been carefully purified by HPLC followed by gel electrophoresis, it is crucial that we address this issue since even a small contamination could generate erroneous data in a site-specific experiment. However, several arguments suggest against such a possibility. First, base substitutions were detected only when SOS functions were induced, suggesting that the contaminant, if any, must also be a SOS-dependent mutagenic lesion. Second, only targeted base substitutions at $G_1$ and $G_2$ were detected, which can be attributed to contaminating oligonucleotides only if the contaminations were different in each sample. This seems unlikely since the chemical adduction of the decamer at $G_1$ and $G_2$ was carried out in the same reaction mixture simultaneously, following which the products were separated and purified. Third, two entirely different syntheses and purifications of the oligonucleotides generated very similar results, making it less likely that the observed base substitutions were originated from a highly mutagenic contaminant.

When the results of this investigation are compared with the same adduct in an identical local sequence and in the same cells, but in ds DNA (*31*), qualitatively they are in agreement on at least two important issues. Both studies show that mutation frequency of (+)-*trans-anti*-B[a]P-$N^2$-dG at $G_1$ is greater than at $G_2$ and that G → T is the major type of mutation. However, there are some notable differences between the studies in ss and ds DNA. When the adduct is at $G_1$, the frequency of base substitutions does not exceed ∼1% in ds DNA (*31*), which is in stark contrast with ∼30% point mutations in ss DNA (Table 3). This reduction in mutagenesis in ds DNA could be the result of many factors. Efficient excision repair in ds DNA is probably a major contributor. In

addition, an exceptionally strong replication block at the adduct site as shown in our investigation may result in a strand bias during replication in ds DNA. Although multiple UV damages were incorporated in the complementary strand by Jelisnky et al. (*31*), this probably does not eliminate the problem of strand bias (see ref 27). There are several other differences between experiments in ds and ss DNA in cells. In ds DNA, both targeted and semi-targeted base pair substitutions were detected, whereas in ss DNA we observed only targeted base substitutions (Table 3). Finally, in ds DNA the adduct at $G_1$ induced G → A and G → C substitutions in addition to G → T transversions (*31*), whereas only the latter were detected in ss DNA. Even though we analyzed only a limited number of progeny, the difference in bias toward G → T substitutions between ss and ds DNA appears to be statistically significant ($p = \sim 0.04$). One explanation of this difference is that the conformational polymorphism of the adduct may be different in ss and ds DNA (*27*). The dissimilar conformation(s) of the lesion, in turn, may influence the types of nucleotide incorporated during translesion synthesis. It is interesting that in a recent study of the same adduct in *E. coli* in which the c-Ha-*ras* protooncogene sequence 5′-TCCTCCTG$_1$G$_2$CCTCTC was used in a single-stranded vector, Moriya et al. detected mutation frequencies of 19% and 3% at $G_1$ and $G_2$, respectively (*44*). Despite differences between the study by Moriya et al. (*44*) and this investigation, a 5′-pyr-$G_1$-$G_2$-pyr sequence was employed in both the studies, and it is noteworthy that the frequency of G → T transversions in each case was much higher when the adduct was located at $G_1$. On the basis of these results, it is tempting to speculate that the conformation of this adduct in a 5′-pyr-$G_1$-$G_2$-pyr sequence is such that dAMP incorporation by *pol* III is much more favorable when the adduct is at $G_1$ compared to the same at $G_2$. Detailed structural analysis of DNA containing (+)-*trans*-*anti*-B[a]P-$N^2$-dG might be able to shed light on this type of critical issues. Regardless of the mechanism of mutagenesis, these data taken together strongly argue that the mutational consequence of (+)-*trans*-*anti*-B[a]P-$N^2$-dG is highly dependent upon the DNA sequence context. In addition, mutagenesis of this adduct in ss DNA is significantly different from that in ds DNA.

**Acknowledgment.** The project was supported by the National Institute of Environmental Health Sciences Grant ES07946 to A.K.B. and Grant ES03775 to E.L.L. The portion of the work performed at NYU was supported by a grant from the Office of Health and Environmental Research, Department of Energy (Grant DE-FGO2-86ER60405) to N.E.G.

## References

(1) Harvey, R. G. (1991) *Polycyclic aromatic hydrocarbons: Chemistry and cancer*, Cambridge University Press, Cambridge, U.K.

(2) Sims, P., Grover, P. L., Swaisland, A., Pal, K., and Hewer, A. (1974) Metabolic activation of benzo[*a*]pyrene proceeds by a diol-epoxide. *Nature* **252**, 326−328.

(3) Yang, S. K., McCourt, D. W., Roller, P. P., and Gelboin, H. V. (1976) Enzymatic conversion of benzo[*a*]pyrene leading predominantly to the diol-epoxide r-7,t-8-dihydroxy-t-9,10-oxy-7,8,9,10-tetrahydobenzo[*a*]pyrene through a single enantiomer of r-7,t-8-dihydroxy-7,8-dihydobenzo[*a*]pyrene. *Proc. Natl. Acad. Sci. U.S.A.* **73**, 2594−2598.

(4) Kapitulnik, J., Wislocki, P. G., Levin, W., Yagi, H., Thakker, D. R., Akagi, H., Koreeda, M., Jerina, M., and Conney, A. H. (1978) Marked differences in the carcinogenic activity of optically pure (+)- and (−)-*trans*-7,8-dihydroxy-7,8-dihydrobenzo[*a*]pyrene in newborn mice. *Cancer Res.* **38**, 2661−2665.

(5) Thakker, D. R., Yagi, H., Lu, A. Y. H., Levin, W., Conney, A. H., and Jerina, D. M. (1976) Metabolism of benzo[*a*]pyrene. IV. Conversion of (±)-*trans*-7,8-dihydroxy-7,8-dihydrobenzo[*a*]pyrene to the highly mutagenic 7,8-diol-9,10-epoxides. *Proc. Natl. Acad. Sci. U.S.A.* **73**, 3381−3385.

(6) Buening, M. K., Wislocki, P. G., Levin, W., Yagi, H., Thakker, D. R., Akagi, H., Koreeda, M., Jerina, D. M., and Conney, A. H. (1978) Tumorigenicity of the optical enantiomers of the diastereomeric benzo[*a*]pyrene 7,8-diol-9,10-epoxides in newborn mice: exceptional activity of (+)-7$\beta$,8α-dihydroxy-9α,10α-epoxy-7,8,9,10-tetrahydrobenzo[*a*]pyrene. *Proc. Natl. Acad. Sci. U.S.A.* **75**, 5358−5361.

(7) Slaga, T. J., Bracken, W. J., Gleason, G., Levin, W., Yagi, H., Jerina, D. M., and Conney, A. H. (1979) Marked differences in the skin tumor-initiating activities of the optical enantiomers of the diastereomeric benzo[*a*]pyrene 7,8-diol-9,10-epoxides. *Cancer Res.* **39**, 67−71.

(8) Wood, A. W., Chang, R. L., Levin, W., Yagi, H., Thakker, D. R., Jerina, D. M., and Conney, A. H. (1977) Differences in mutagenicity of the optical enantiomers of the diastereomeric benzo[*a*]-pyrene 7,8-diol-9,10-epoxides. *Biochem. Biophys. Res. Commun.* **77**, 1389−1396.

(9) Brookes, P., and Osborne, M. R. (1982) Mutation in mammalian cells by stereoisomers of *anti*-benzo[*a*]pyrene diol epoxide in relation to the extent and nature of the DNA reaction product. *Carcinogenesis* **3**, 1223−1226.

(10) Burgess, J. A., Stevens, C. W., and Fahl, W. E. (1985) Mutation at separate gene loci in *Salmonella typhimurium* TA 100 related to DNA nucleotide modification by stereoisomeric benzo[*a*]pyrene 7,8-diol-9,10-epoxides. *Cancer Res.* **45**, 4257−4262.

(11) Stevens, C. W., Bouck, N., Burgess, J. A., and Fahl, W. E. (1985) Benzo[*a*]pyrene diol epoxide: different mutagenic efficiency in human and bacterial cells. *Mutat. Res.* **152**, 5.

(12) Weinstein, I. B., Jeffrey, A. M., Jennette, K. W., Blobstein, S. H., Harvey, R. G., Harris, C., Autrup, H., Kasai, H., and Nakanishi, K. (1976) Benzo[*a*]pyrene diol epoxides as intermediates in nucleic acid binding *in vitro* and *in vivo*. *Science* **193**, 592−594.

(13) Jeffrey, A. M., Jennette, K. W., Blobstein, S. H., Weinstein, I. B., Beland, F. A., Harvey, R. G., Kasai, H., Miura, I., and Nakanishi, K. (1976) Benzo[*a*]pyrene-nucleic acid derivative found *in vivo*: Structure of a benzo[*a*]pyrenetetrahydrodiol epoxide-guanosine adduct. *J. Am. Chem. Soc.* **98**, 5714−5715.

(14) Osborne, M. R., Beland, F. A., Harvey, R. G., and Brookes, P. (1976) The reaction of (±)-7α,8$\beta$-dihydroxy-9$\beta$,10$\beta$-epoxy-7,8,9,10-tetrahydrobenzo[*a*]pyrene with DNA. *Int. J. Cancer* **18**, 362−368.

(15) Osborne, M. R., Harvey, R. G., and Brookes, P. (1978) The reaction of *trans*-7,8-dihydroxy-*anti*-9,10-epoxy-7,8,9,10-tetrahydrobenzo-[*a*]pyrene with DNA involves attack at the N7-position of guanine moeities. *Chem.-Biol. Interact.* **20**, 123−130.

(16) Cheng, S. C., Hilton, B. D., Roman, J. M., and Dipple, A. (1989) DNA adducts from carcinogenic and noncarcinogenic enantiomers of benzo[*a*]pyrene dihydrodiol epoxide. *Chem. Res. Toxicol.* **2**, 334−340.

(17) Sayer, J. M., Chadha, A., Agarwal, H. S. K., Yeh, H. J. C., Yagi, H., and Jerina, D. M. (1991) Covalent nucleoside adducts of benzo-[*a*]pyrene 7,8-diol 9,10-epoxides: structural reinvestigation and characterization of a novel adenosine adduct on the ribose moiety. *J. Org. Chem.* **56**, 20−29.

(18) Eisenstadt, E., Warren, J., Porter, J., Atkins, D., and Miller, J. H. (1982) Carcinogenic epoxides of benzo[*a*]pyrene and cyclopenta-[cd]pyrene induce base substitutions via specific transversions. *Proc. Natl. Acad. Sci. U.S.A.* **79**, 1945−1949.

(19) Yang, J.-L., Mahar, V. M., and McCormick, J. J. (1987) Kinds of mutations formed when a shuttle vector containing adducts of (±)-7$\beta$,8α-dihydroxy-9α,10α-epoxy-7,8,9,10-tetrahydrobezo[*a*]py-rene replicates in human cells. *Proc. Natl. Acad. Sci. U.S.A.* **84**, 3787−3791.

(20) Chen, R.-H., Mahar, V. M., and McCormick, J. J. (1990) Effects of excision repair by diploid human fibroblasts on the kinds and locations of mutations induced by (+/-)-7$\beta$,8α-dihydroxy-9α,10α-epoxy-7,8,9,10-tetrahydrobenzo[*a*]pyrene in the coding region of HPRT gene. *Proc. Natl. Acad. Sci. U.S.A.* **87**, 8680−8684.

(21) Wei, S.-J. C., Chang, R. L., Wong, C.-Q., Bhachech, N., Cui, X. X., Hennig, E., Yagi, H., Sayer, S. M., Jerina, D. M., Preston, B. D., and Conney, A. H. (1991) Dose-dependent differences in the profile of mutations induced by an ultimate carcinogen from benzo[*a*]pyrene. *Proc. Natl. Acad. Sci. U.S.A.* **88**, 11227−11230.

(22) Wei, S.-J. C., Chang, R. L., Bhachech, N., Cui, X. X., Merkler, K. A., Wong, C.-Q., Hennig, E., Yagi, H., Sayer, S. M., Jerina, D. M., and Conney, A. H. (1993) Dose-dependent differences in the profile of mutations induced by (+)-7*R*,8*S*-dihydroxy-9*S*,10*R*-epoxy-7,8,9,10-tetrahydrobezo[*a*]pyrene in the coding region of the hypoxanthine (guanine) phosphoribosyltransferase gene in Chinese hamster V79 cells. *Cancer Res.* **53**, 3294−3301.

(23) Rodriguez, H., and Loechler, E. L. (1993) Mutational specificity of the (+)-*anti*-diol epoxide of benzo[*a*]pyrene in a *supF* gene of an *Escherichia coli* plasmid: DNA sequence context influences hot spots, mutagenic specificity and the extent of SOS enhancement of mutagenesis. *Carcinogenesis* **14**, 373−383.

(24) Rodriguez, H., and Loechler, E. L. (1993) Mutagenesis by the (+)-*anti*-diol epoxide of benzo[*a*]pyrene: What controls mutagenic specifity? *Biochemistry* **32**, 1759−1769.

(25) Basu, A. K., and Essigmann, J. M. (1988) Site-specifically modified oligodeoxynucleotides as probes for the structural and biological effects of DNA damaging agents. *Chem. Res. Toxicol.* **1**, 1−18.

(26) Singer, B., and Essigmann, J. M. (1991) Site-specific mutagenesis: retrospective and prospective. *Carcinogenesis* **12**, 949−955.

(27) Loechler, E. L. (1996) The role of adduct site-specific mutagenesis in understanding how carcinogen-DNA adducts cause mutations: perspective, prospects and problems. *Carcinogenesis* **17**, 895−902.

(28) Mackay, W., Benasutti, M., Droulin, E., and Loechler, E. L. (1992) Mutagenesis by (+)-*anti*-B[a]P-$N^2$-Gua, the major adduct of activated benzo[*a*]pyrene, when studied in an *Escherichia coli* plasmid using site-directed methods. *Carcinogenesis* **13**, 1415−1425.

(29) Hruszkewycz, A. M., Canella, K. A., Peltonen, K., Kotrappa, L., and Dipple, A. (1992) DNA polymerase action on benzo[*a*]pyrene-DNA adducts. *Carcinogenesis* **13**, 2347−2352.

(30) Shibutani, S., Margulis, L. A., Geacintov, N. E., and Grollman, A. P. (1993) Translesional synthesis on a DNA template containing a single stereoisomer of dG-(+)- and dG-(−)-*anti*-BPDE (7,8-dihydroxy-*anti*-9,10-epoxy-7,8,9,10-tetrahydrobenzo[*a*]pyrene). *Biochemistry* **32**, 7531−7541.

(31) Jelinsky, S. A., Liu, T.-M., Geacintov, N. E., and Loechler, E. L. (1995) The major, $N^2$-Gua adduct of the (+)-*anti*-benzo[*a*]pyrene diol epoxide is capable of inducing G → A and G → C, in addition to G → T, mutations. *Biochemistry* **34**, 13545−13553.

(32) Malia, S. A., Vyas, R. R., and Basu, A. K. (1996) Site-specific frame-shift mutagenesis by the 1-nitropyrene adduct N-(deoxyguanosin-8-yl)-1-aminopyrene located in the $(CG)_3$ sequence: Effects of SOS, proofreading, and mismatch repair. *Biochemistry* **35**, 4568−4577.

(33) Sambrook, J., Fritsch, E. F., and Maniatis, T. (1989) In *Molecular Cloning: A Laboratory Manual*, Cold Spring Harbor Laboratory Press, Cold Spring Harbor, NY.

(34) Basu, A. K., Hanrahan, C. J., Malia, S. A., Kumar, S., Bizanek, R., and Tomasz, M. (1993) Effect of site-specifically located mitomycin C-DNA monoadducts on *in vitro* DNA synthesis by DNA polymerases. *Biochemistry* **32**, 4708−4718.

(35) Boosalis, M. S., Petruska, J., and Goodman, M. F. (1987) DNA polymerase insertion fidelity: Gel assay for site-specific kinetics. *J. Biol. Chem.* **262**, 14689−14696.

(36) Clark, J. M. (1988) Novel non-templated nucleotide addition reactions catalyzed by procaryotic and eucaryotic DNA polymerases. *Nucleic Acids Res.* **16**, 9677−9686.

(37) Moore, P. D., Bose, K. K., Rabkin, S. D., and Strauss, B. S. (1981) Sites of termination of *in vitro* DNA synthesis on ultraviolet- and *N*-acetylaminofluorene-treated $\phi$x 174 templates by prokaryotic and eukaryotic DNA polymerases. *Proc. Natl. Acad. Sci. U.S.A.* **78**, 110−114.

(38) Strauss, B. S., Rabkin, S., Sagher, D., and Moore, P. (1982) The role of DNA polymerase in base substitution mutagenesis on non-instructional templates *Biochimie* **64**, 829−838.

(39) Strauss, B. S. (1985) Translesion DNA synthesis: polymerase response to altered nucleotides. *Cancer Surv.* **4**, 493−516.

(40) Banerjee, S. K., Christensen, R. B., Lawrence, C. W., and LeClerc, J. E. (1988) Frequency and spectrum of mutations produced by a single *cis-syn* thymine-thymine cylobutane dimer in a single-stranded vector. *Proc. Natl. Acad. Sci. U.S.A.* **85**, 8141−8145.

(41) Lawrence, C. W., Borden, A., Banerjee, S. K., and LeClerc, J. E. (1990) Mutation frequency and spectrum resulting from a single abasic site in a single-stranded vector. *Nucleic Acids Res.* **18**, 2153−2157.

(42) Cosman, M., de los Santos, C., Fiala, R., Hingerty, B. E., Singh, S., Ibanez, V., Margulis, L., Live, D., Geacintov, N. E., Broyde, S., and Patel, D. J. (1992) Solution conformation of the major adduct between the carcinogen (+)-*anti*-benzo[*a*]pyrene diol epoxide and DNA. *Proc. Natl. Acad. Sci. U.S.A.* **89**, 1914−1918.

(43) Chary, P., Latham, G. J., Robberson, D. L., Kim, S. J., Han, S., Harris, C. M., Harris, T. M., and Lloyd, R. S. (1995) *In vivo* and *in vitro* replication consequences of stereoisomeric benzo[*a*]pyrene-7,8-dihydrodiol 9,10-epoxide adducts on adenine $N^6$ at the second position of N-*ras* codon 61. *J. Biol. Chem.* **270**, 4990−5000.

(44) Moriya, M., Spiegel, S., Farnandes, A., Amin, S., Liu, T., Geacintov, N., and Grollman, A. P. (1995) Fidelity of translesional synthesis past benzo[*a*]pyrene diol epoxide-2′-deoxyguanosine DNA adducts: marked effects of host cell, sequence context and chirality. *Biochemistry* **35**, 16646−16651.

TX9601925